RADIOGENIC HEAT PRODUCTION IN THE MOON: CONSTRAINTS FROM PLAGIOCLASE-MELT TRACE ELEMENT PARTITIONING EXPERIMENTS. J. de Vries[1,2], W. van Westrenen[1] and A. van den Berg[2], [1]VU University Amsterdam, Netherlands, j.de.vries@vu.nl, [2]Utrecht University, Netherlands

Introduction: Accurate knowledge of global heat budgets is essential for the development of planetary thermal evolution models. In contrast to Earth, the lunar heat budget is at present poorly constrained. Only four heat flow measurements have been performed on the Moon [1], and the concentrations of U, Th and K in the Moon are not well constrained. Here, we explore a method of estimating radiogenic heat production in the Moon, and its depth distribution, based on combining recent observations of the surface concentrations of U, Th and K in the highlands regions of the Moon with experimental constraints on the distribution of these elements between anorthositic plagioclase and silicate melt at high temperature.

Background: Remote sensing data on the composition of the lunar surface, combined with data from samples returned with the Apollo and Luna missions and meteorite data, has led to improved estimates of the potassium, thorium and uranium concentrations of the lunar surface, e.g. [2-6]. Most studies to date have focused on the resulting concentrations of radiogenic heat producing elements in the Procellarum KREEP terrane on the lunar near side, which shows pronounced enrichments in K, U and Th concentrations due to the influence of the enriched KREEP source. Our focus here is on the concentrations of the main heat producing elements derived for the Feldspathic Highlands Terrane (FHT), composed mostly of anorthite-rich plagioclase, as the Lunar Magma Ocean (LMO) concept provides a direct link between surface remote sensing data and the Moon's interior heat budget. These data, together with mineral-melt partition coeffients for Th, U and K constrain the concentrations of these elements in the main lunar silicate reservoirs, from which the bulk Moon concentrations can be determined.

Crystallisation of the LMO resulted in a layered mantle with olivine and orthopyroxene-rich layers at the bottom, followed by clinopyroxene-rich materials and a dense ilmenite-rich layer at shallow depth below the plagioclase flotation crust [7]. To combine surface concentration observations with this petrological model for LMO crystallisation and thus provide information about the Moon's heat budget, information is required on the partitioning behaviour of U, Th and K between plagioclase and melt. Although some preliminary models for the behaviour of U and Th in plagioclase-melt systems were developed in the past [8], the experimental database used for these models is small -

mostly due to the fact that on Earth, plagioclase is not a relevant reservoir for these elements.

Previous studies on trace element incorporation into plagioclase [9-14] did not focus on the radioactive elements Th and U (although some of these studies did include these elements in their experiments). As a result the spread in partition coefficients for U and Th is very large. For U, plagioclase-melt partition coefficients reported in the literature vary from 0.00004 to 0.5. For Th, the variation also covers several orders of magnitude ($0.0004 < D_{Th} < 0.38$).

We experimentally determined the partitioning of U, Th, K and a suite of other trace elements between anorthite-rich plagioclase and silicate melt at high temperature and atmospheric pressure. The lattice strain model [15] was used to rationalise plagioclase-melt partition coefficients for 1+, 2+, 3+ and 4+ trace elements. Our data are used to provide new estimates for the concentrations of U, Th and K in the lunar interior, which can serve as input parameters for models of lunar thermo-chemical evolution.

Methods: To separate the effect of composition from the possible effects of temperature and pressure, we chose compositions in the anhydrous simple system anorthite-albite-diopside, enabling synthesis of a range of plagioclase-melt pairs at a constant pressure of 1 bar and near-constant temperature of 1200-1230 °C with different compositions. Experiments were performed in air in a box furnace. Run products (Fig. 1) were analysed by electron microprobe for major elements and laser ablation-ICP-MS for trace elements using methods described elsewhere [16].
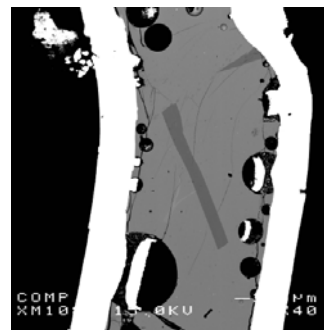

Fig. 1. Back-scattered electron image of typical polished run product. Plagioclase laths in dark grey, co-existing glass in light grey, Pt capsule in white.

Results: A range of plagioclase compositions between An58 and An81 was produced, enabling us to study the influence of the plagioclase anorthite content on partition coefficients. Our results for univalent, divalent and trivalent trace elements (not shown) are in

good agreement with previous plagioclase-melt partitioning experiments performed at similar conditions. Data for 1+, 2+, and 3+ elements are all amenable to lattice strain modeling treatment, and resulting lattice strain model parameters are in exellent agreement with previous work (not shown). We do not find any significant effect of plagioclase composition on D values. Figure 2 shows our partitioning values for Zr, Hf, U, and Th, together with lattice strain model fits. Fits to D_{Zr}, D_{Hf} and D_{Th} result in very similar ideal ionic radii r_0 values for all experiments, with a mean value of 0.925 Å.
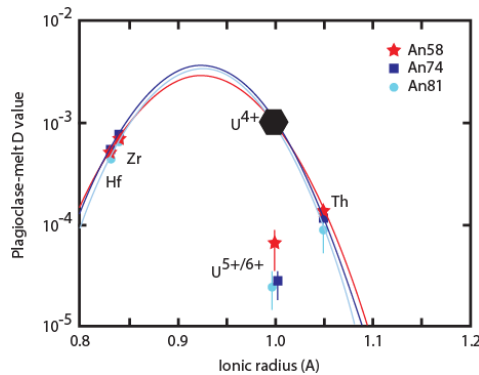

Fig 2. Measured plagioclase-melt D values for Zr, Hf, U and Th (small symbols), lattice strain models(curves) and predicted U4+ partition coefficient (large symbol).

Measured D_U values consistently fall significantly below the best-fit curves. It is important to note that our experiments were performed in air, in the absence of an oxygen fugacity buffer. At these conditions (log fO_2 approximately -0.7), uranium is not quadruvalent, but present mostly as pentavalent or hexavalent cations [17]. It is therefore not surprising that our U partitioning data do not fit the parabolic trends defined by the Zr, Hf and Th data. The fact that our measured D_U values lie significantly below the curve derived from the other elements is consistent with the fact that D for trace elements with charges >3+ decrease with increasing charge [18]. Our fits make it possible to estimate a partition coefficient for U^{4+} of approximately 0.00103. This estimate is required as, at the oxygen fugacity in the Moon, uranium is likely to be present in the 4+ state. The predicted D is an order of magnitude larger the the measured D. The fits indicate that the U^{4+} D is independent of plagioclase composition, enabling use of this value for models of lunar magmatic systems where the exact plagioclase composition and its variation are not perfectly known.

Implications for lunar heat budget: Our data on partitioning of U, Th and K between plagioclase and melt, combined with partitioning data for these elements in other minerals and an LMO crystallization sequence, can be used to estimate the total lunar heat budget. A sample calculation, using Apollo-derived surface plagioclase concentrations of 84 ppb for Th and 13 ppb for U, is shown in Fig. 3.
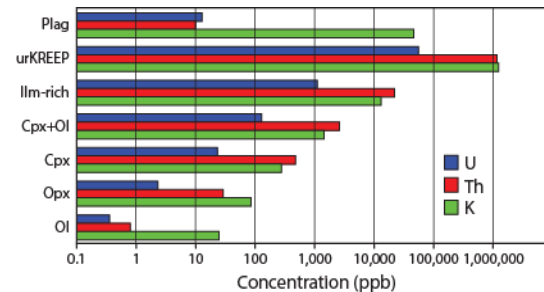

Fig 3.Sample calculation of spatial distribution of K, U and Th after solidification of the LMO using our plagioclase-melt D values for U and Th (Fig. 2)

A major result from our modeling is that resulting estimated bulk Moon Th and U levels are unrealistically high. This indicates that plagioclase Th and U concentrations as taken from Apollo rock measurements, cannot represent concentrations in true primary plagioclase that crystallised from the LMO. To improve the calculation on heat production in the lunar minerals, accurate knowledge of trace element concentrations for pure LMO-derived anorthosites is essential, likely requiring new sample return missions. Furthermore, additional work on partitioning of 4+ elements under reducing conditions is needed to to determine the Th and U^{4+} D values for lunar applications with higher accuracy.

References: [1] Langseth M. et al. (1976) *LPSC 7*, 3143 [2] Takeda, H. et al. (2006) *EPSL 247*, 171 [3] Prettyman T. et al. (2007) *JGRP 111*, E12007 [4] Yamashita N. et al. (2010) *GRL 37*, L10201 [5] Kobayashi S. et al. (2010) *SSR 154*, 193 [6] Jolliff B.L. et al. (2011) *Nat Geo 4*, 566 [7] Snyder, G. et al. (1992) *GCA 56*, 3809 [8] Blundy J.D. and Wood B.J. (2003), *RMG 52*, 59 [9] Drake M. and Weill D. (1975) *GCA 39*, 689 [10] Bindeman I. et al. (1998) *GCA 62*, 1175 [11] Bindeman I. and Davis A. (2000) *GCA 64*, 2863 [12] Miller S. et al. (2006) *GCA 70*, 4258 [13] Aigner-Torres M. et al. (2007) *CMP 153*, 647 [14] Tepley III F. et al. (2010) *Lithos 118*, 82 [15] Blundy J.D. and Wood B.J. (1994) *Nature 372*, 452 [16] Van Kan Parker M. et al. (2011) *GCA 75*, 4179 [17] Berry A. et al. (2008) *GCA 12S1*, A79 [18] Wood B.J. and Blundy J.D. (2001) *EPSL 188*, 59.